Graphene-ZnO NWs film for large-area UV photodetector

Fengyuan Liu[1], Nivasan Yogeswaran[1], Carlos García Núñez[1], Duncan Gregory[2] and Ravinder Dahiya[1*]
[1]School of Engineering, University of Glasgow
[2]School of Chemistry, University of Glasgow
[*]Correspondence to: Ravinder.Dahiya@glasgow.ac.uk

***Abstract*— This work demonstrates large-area (~4cm^2) UV photodetector by heterogenous integration of graphene-ZnO nanowires (NWs) using a facile and cost-effective method. Owing to the low and wavelength-independent light absorption, it is difficult to obtain high-performance graphene-based photodetector (PD). The research presented here addresses this challenge by integrating light sensitive material (ZnO) on graphene. The huge sensitivity of ZnO NWs to UV light, combined with the high carrier mobility of graphene, enable the UV PD with a photoresponse up to 2100 A/W, and fast response times down to millisecond.**

Keywords*— *Graphene; ZnO NW; Photodetector; Heterogeneous integration; large-area electronics

I. INTRODUCTION

Since its first isolation in 2004 [1], graphene has attracted great interest because of its potential use in many applications, including electronics, optoelectronics, photonics, photovoltaics, and e-skin etc [2, 3]. Due to properties such as ultra-high carrier mobility and tunable optical properties by modulating the Fermi level, graphene has been extensively investigated for photodetection [4]. As a single atomic layer thick material, graphene also shows outstanding flexibility and stretchability, which holds great promise for developing novel optoelectronic devices with diverse morphological features [5, 6]. However, the small and constant light absorption (2.3%) over a long wavelength range is a major drawback when it comes to using graphene for photodetection (although the same feature makes graphene attractive for the development of high-performance transparent electronics [5]). A number of strategies have been proposed and demonstrated to enable the photodetection based on graphene and these include photovoltaic effect [7, 8], photo-thermoelectric effect [9] and photogating effect [10], etc. Among these the integration of graphene with light sensitive materials (photogating effect) such as ZnO, PbS, and CdS etc. has been suggested as promising strategy to realize a high sensitive photoresponse covering the wavelength range from UV to IR. Integration of such materials allows to overcome graphene's limited ability to absorb light. Many of the graphene and light sensitive materials-based proof-of-concept devices have shown competing performance with respect to currently mature PD technology [4].

Despite rapid progress in graphene research, the realization of large-area hybrid integration of graphene and the light-sensitive materials for device application is still challenging. The problem at present are majorly coming from two aspects: First, the large-area processing of graphene for device application of high-performance is challenging with existing complementary-metal-oxide-semiconductor (CMOS) based technology (specifically UV photolithography) due to a serious photoresist residue problem [11]. Second, the uniform hybrid integration of graphene and other materials over large-area is not straight forward. Many extrinsic factors such as wrinkles and polymer residues may disturb the uniformity of the hybrid integration.

In this work, we present a novel and cost-effective strategy to integrate single layer graphene and ZnO NWs. Taking advantages of high sensitivity and selectivity of ZnO NWs to UV light [12, 13] and the high mobility of graphene, the hybrid film from them works as a UV PD with fast response down to millisecond. Moreover, the method developed here allowed the fabrication of PDs array over large areas (4 cm^2). The fabrication is only limited by the sample size and can be easily extended to wafer-scale by using the recently developed large-area graphene synthesis and transfer techniques [14, 15]. We believe the adopted method is promising for realizing large-area, and cost-effective graphene based optoelectronic devices.

This paper is organised as follows: The steps related to device fabrication and hybrid integration are explained in Section II. This is followed by results and discussion in Section III and a summary of key outcomes in Section IV.

II. DEVICE FABRICATION

A. Graphene Field-effect transistor (FET) Fabrication

The fabrication steps of UV PDs based on graphene-ZnO NWs are schematically presented in Figure 1. PDs were fabricated on SiO_2 (300 nm)/Si substrates (Figure 1a). Source and drain electrodes, consisting of Ti (3 nm)/Au (80 nm), were defined by photolithography, metal evaporation and lift-off process (Figure 1b). After that, a CVD graphene film was transferred onto the substrate with pre-patterned electrodes by using the conventional PMMA-assisted transfer method (Figure 1c) [16]. The PMMA supporting layer was then removed by putting the sample into acetone overnight. The surface cleanliness of graphene was confirmed by atomic-force microscope (AFM) characterization, which is discussed in the next section. The contact formed between the transferred graphene and pre-patterned electrode lies in the van der Waals interaction regime. Despite the weak nature of van der Waals force, the value of contact resistance between graphene and electrodes in this scenario is still modest (~400Ω×µm at high carrier density, obtained by an individual four terminal measurement). This value is also consistent with previous report [17]. The fabrication method presented above prevents the direct photolithography process on graphene, offering a cost-effective

This work was supported in part by the EPSRC Engineering Fellowship for Growth-PRINTSKIN (EP/M002527/1).

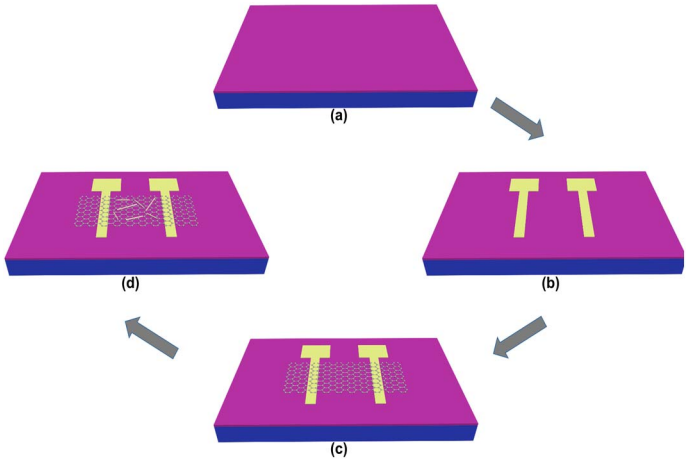

Fig. 1: 3D schema of graphene-ZnO NW based UV PD fabrication steps. (a) SiO_2 (300 nm)/Si substrates; (b) substrate with pre-patterned source and drain electrodes; (c) graphene transferred onto the substrate with pre-patterned electrodes; (d) graphene-ZnO NWs hybrid film-based PD.

alternative strategy to realize the contact for fabricating graphene-based device.

B. Integration of ZnO NWs on Graphene FET

ZnO NWs were dispersed in IPA with a concentration of 0.25 mg/ml. Thereafter, a 100 µl volume of NWs solution was spin-coated on top of the graphene surface (Figure 1d). The density of ZnO NWs coating the graphene surface was controlled by the number of spin-coating cycles and the NW solution concentration. For each cycle, 100 µL dispersion was drop-casted on top of the sample surface (~4 cm^2) and then spin-coated at the speed of 2000 rpm for 60s. This process was repeated for 15 times to achieve a high density of ZnO NWs.

III. Results and Dicussion

A. Characterization of the graphene-ZnO NWs hybrid film

The graphene was characterized by AFM before and after the spin-coating. As shown in Fig. 2a, the as-transferred graphene shows a rather clean surface with little PMMA residue on the surface. After the spin-coating process, the NWs were integrated on top of graphene with a high-quality interface as no obvious polymer residue can be observed at the interface between graphene and ZnO (Fig. 2b). This is crucial for the carrier transfer between ZnO NW and graphene. The hybrid film was also characterized by Raman spectroscopy. Result shows a typical graphene signal with no obvious D peak (Fig. 2c), which further confirms the feasibility of proposed method for heterogeneous integration of high-quality graphene-ZnO NW over large area without using notoriously non-manufacturing techniques.

The density of ZnO NWs after their spin-coating on graphene has been studied by means of scanning electron microscope (SEM). From this analysis, randomly oriented NWs were found to cover uniformly the entire surface of graphene FET (Fig. 2d). The density of NWs measured on top of graphene channel area was found to be uniform over different devices, with an average value of around 0.08 NWs per µm^2. The excellent uniformity achieved over different devices is probably

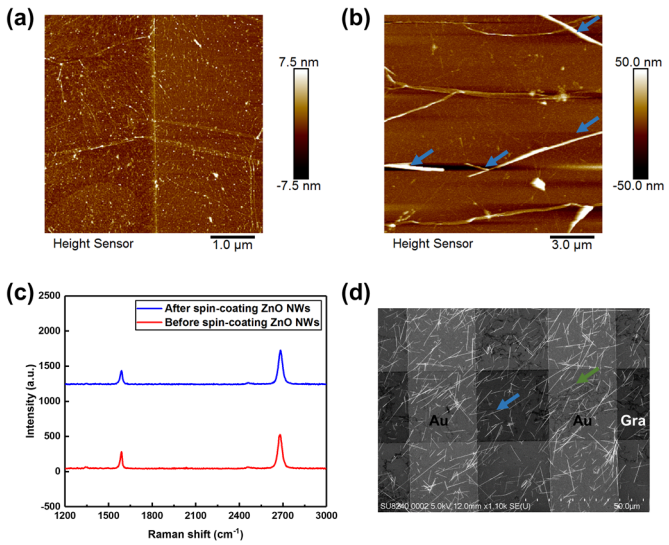

Fig. 2: The AFM image before (a) and after (b) spin-coating ZnO NWs. (c) the Raman and (d) SEM characterization of graphene-ZnO NWs hybrid film. The blue (green) arrow indicates the ZnO NWs on graphene channel (contact).

due to the large number of used spin-coating cycles and this shows the feasibility and reproducibility of the overall process. It should be also noted that there are a large number of NWs coated around the graphene-metal contacts regions. Since the graphene was transferred on top of Au electrodes, the NWs at that region can also have charge transfer between the graphene underneath. This could influence the graphene-metal contact under UV illumination, which is discussed later in this paper.

B. Photoresponse of graphene-ZnO NWs hybrid film

The as-fabricated UV PD was measured in the ambient atmosphere and under different power of illuminations. In dark conditions, the Dirac point of graphene FET was at ~32.5V, indicating a p-type doping of the channel region. Under UV illumination using a UV LED (power of 3.4 µW/cm^2), the Dirac point remained almost unchanged. The two-transfer curve shows a slightly shift, resulting in a net photoresponse. (Fig. 3a) However, we do notice that there is an unreliability from the gate induced charge while applying the gate voltage [18], as a result, the later discussion is based on the result obtained at $V_g=0$.

The response time of graphene-ZnO NW UV PDs was analysed by transient time measurements under periodic UV illumination. As can be seen from Fig. 3b, with the periodic switching of the UV illumination, the device shows a robust and reversible switching response. The rise and decay time were measured to be less than 30ms and 80ms as shown in Fig. 3c and 3d, respectively. The responsivity, R was determined using equation $R=I_{ph}/P$, where the I_{ph} represents the measured photocurrent and P indicates the illumination power. Then we studied the relationship between photoresponse and the illumination power. As can be seen from Fig. 3e, the photoresponse increases while the illumination power decreases. The maximum photoresponse we obtained in our experiment is ~2100 A/W. This figure of merit can be further improved by decreasing the illumination power.

Under illumination, large number of electron-hole pairs are generated in ZnO NWs (Fig. 3f). Since there are many surface

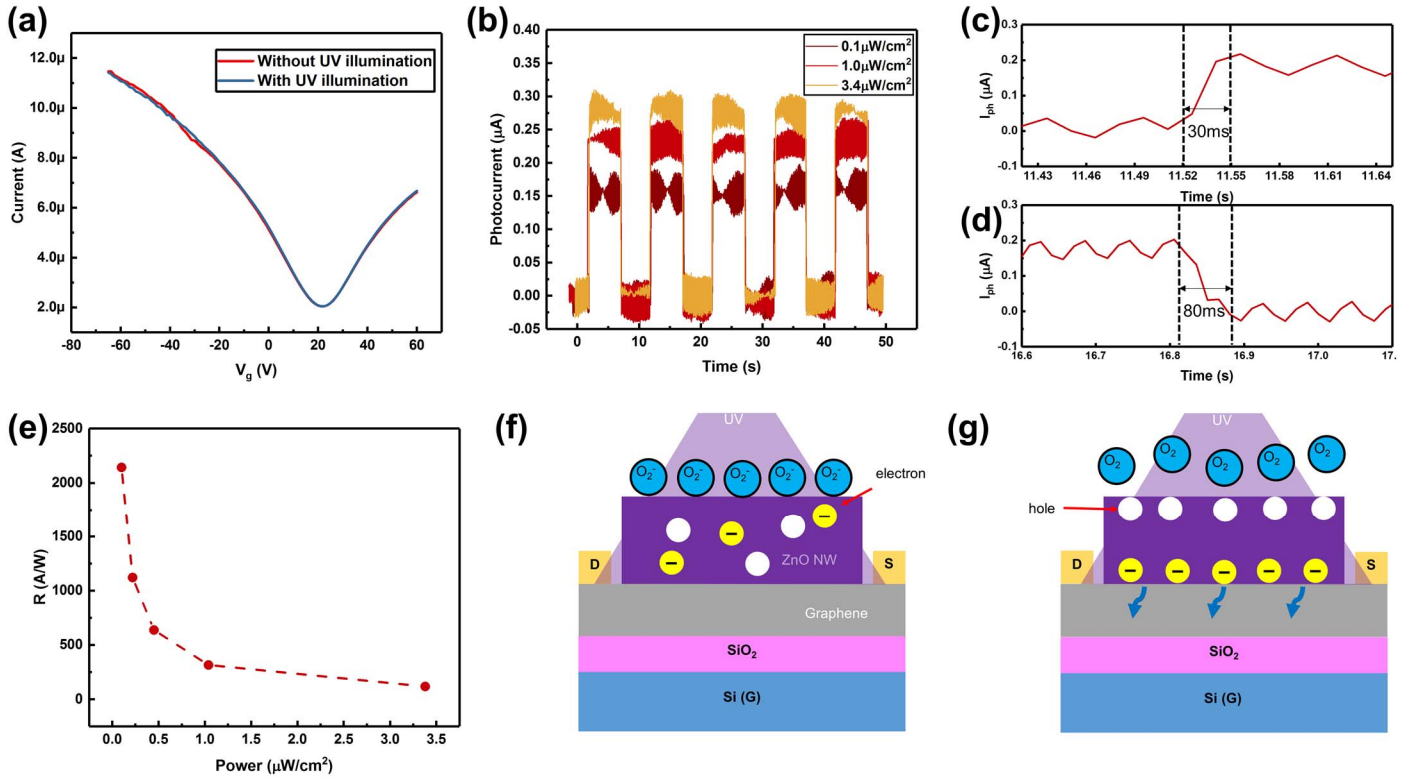

Fig. 3: (a) The transfer curve of the device measured under the environment with and without UV illumination. (b) the transient time measurements under periodic UV illumination, (c) and (d) the zoomed in transient time measurement showing the estimation of the rise and decay time, respectively. (e) the relationship between illumination power and the photoresponse. (f) the schema of photoresponse mechanism, showing the generation of electron-hole pairs in ZnO NW immediately after the UV illumination (g) the schema of photoresponse mechanism, showing the releasing of the trapped oxygen groups from the surface of NW and the transfer of the electrons from NW to graphene.

states at the NWs, the generated holes are trapped, releasing the adsorbed oxygen from the ZnO NW surface to the air. The unpaired photoelectrons are transferred to graphene lattice under the influence of the built-in electric field, leading to the recombination with the carriers in graphene lattice (Fig. 3g). In this scenario, the total carrier density varies, leading to the net photoresponse. The carrier transfer process, which occurs between ZnO NW and graphene in the device channel region, is believed to dominate the photoresponse process. Such mechanism can be further confirmed by measuring the device under vacuum, which will be one of our future work.

Finally, we briefly discuss the influence of the ZnO NWs from different regions to the photoresponse of the device. As can be seen from Fig. 2d, the spin-coated NWs are located at either graphene channel or the graphene-Au contact. We now focus on the photoresponse contributed from the contact. Under UV illumination, the photo-induced electron are transferred from ZnO NWs to graphene (in contact region) under the built-in electric field. Since the graphene in contact with Au is p-type doped [19], such excess carriers will shift the Fermi level of graphene towards Dirac point. Considering that the number of quantum modes M follows the relationship of $M = (\Delta E_f/\pi\hbar V_f)W$, M should decrease under UV illumination due to the charge transfer from NW to graphene [20]. (The ΔE_f and V_f represent the shift of Fermi level with respect to the Dirac point and the Fermi velocity (~10^6 m/s), respectively). According to Landauer's equation, the contact conductance G is linearly dependent on the number of conduction modes M in graphene as per the equation $G=(4e^2/h)TM$, where T denotes the carrier transmission probability. We thus speculate, under UV illumination, the contact resistance increases. This is another aspect of device response to the UV illumination. We also believe this phenomenon may not be dominating in our device: compared to the carrier transferred to the graphene channel, the carrier transferred to the contact should have a less impact due to a further decay when crossing the graphene-Au tunnel barrier. The transmittance T is always less than 1 in a realistic case [20]. To quantitatively separate the photoresponse originated from the contact, a more detailed experimental study is needed. This can be done by either using a focused UV illumination or a precisely controlled NW distribution on the graphene FET, which will be one of our future study. However, with the existing data, it is enough to demonstrate that the graphene-ZnO NWs hybrid film shows a robust and reliable response to UV illumination.

IV. Conclusion

In conclusion, a facile and cost-effective method is proposed for realizing the graphene-ZnO NWs hybrid film over large-area. The device shows response to UV illumination, with a fast response time down to 30ms and photoresponse up to 2100 A/W. The sensing mechanism of the device is attributed to the photo-induced carrier transfer between the surface of ZnO NW and graphene film. We believe the approach proposed in this paper paves a new way towards the large-area fabrication of graphene-based photodetectors.

V. REFERENCES

[1] K. S. Novoselov, A. K. Geim, S. V. Morozov, D. Jiang, Y. Zhang, S. V. Dubonos, *et al.*, "Electric Field Effect in Atomically Thin Carbon Films," *Science,* vol. 306, pp. 666-669, 2004.

[2] K. S. Novoselov, V. I. Fal′ ko, L. Colombo, P. R. Gellert, M. G. Schwab, and K. Kim, "A roadmap for graphene," *Nature,* vol. 490, p. 192, 2012.

[3] C. G. Núñez, W. T. Navaraj, E. O. Polat, and R. Dahiya, "Energy‐Autonomous, Flexible, and Transparent Tactile Skin," *Advanced Functional Materials,* vol. 27, p. 1606287, 2017.

[4] F. H. L. Koppens, T. Mueller, P. Avouris, A. C. Ferrari, M. S. Vitiello, and M. Polini, "Photodetectors based on graphene, other two-dimensional materials and hybrid systems," *Nature Nanotechnology,* vol. 9, p. 780, 2014.

[5] T. Georgiou, R. Jalil, B. D. Belle, L. Britnell, R. V. Gorbachev, S. V. Morozov, *et al.*, "Vertical field-effect transistor based on graphene–WS 2 heterostructures for flexible and transparent electronics," *Nature nanotechnology,* vol. 8, p. 100, 2013.

[6] K. S. Kim, Y. Zhao, H. Jang, S. Y. Lee, J. M. Kim, K. S. Kim, *et al.*, "Large-scale pattern growth of graphene films for stretchable transparent electrodes," *nature,* vol. 457, p. 706, 2009.

[7] M. Freitag, T. Low, F. Xia, and P. Avouris, "Photoconductivity of biased graphene," *Nature Photonics,* vol. 7, p. 53, 2012

[8] N. Yogeswaran, D. Shakthivel, L. Lorenzelli, V. Vinciguerra, R. Dahiya, "Graphene gold nanoparticle hybrid based near infrared photodetector," IEEE Sensors 2017, Glasgow, UK, Nov 2017

[9] N. M. Gabor, J. C. W. Song, Q. Ma, N. L. Nair, T. Taychatanapat, K. Watanabe, *et al.*, "Hot Carrier–Assisted Intrinsic Photoresponse in Graphene," *Science,* vol. 334, pp. 648-652, 2011.

[10] W. Guo, S. Xu, Z. Wu, N. Wang, M. Loy, and S. Du, "Oxygen‐Assisted Charge Transfer Between ZnO Quantum Dots and Graphene," *Small,* vol. 9, pp. 3031-3036, 2013.

[11] S. Rahimi, L. Tao, S. F. Chowdhury, S. Park, A. Jouvray, S. Buttress, *et al.*, "Toward 300 mm Wafer-Scalable High-Performance Polycrystalline Chemical Vapor Deposited Graphene Transistors," *ACS Nano,* vol. 8, pp. 10471-10479, 2014.

[12] C. G. Nunez, F. Liu, W. T. Navaraj, A. Christou D. Shakthivel, and R. Dahiya, "Heterogeneous Integration of Contact-printed Semiconductor Nanowires for High Performance Devices on Large Areas," Microsystems & Nanoengineering, (in press)

[13] C. G. Nunez, A. Vilouras, W. T. Navaraj, F. Liu, R. Dahiya, "ZnO Nanowires based Flexible UV Photodetector System for Wearable Dosimetry," IEEE Sensors J., 2018. (in press)

[14] E. O. Polat, O. Balci, N. Kakenov, H. B. Uzlu, C. Kocabas, and R. Dahiya, "Synthesis of Large Area Graphene for High Performance in Flexible Optoelectronic Devices," *Scientific Reports,* vol. 5, p. 16744, 2015.

[15] J. Song, F.-Y. Kam, R.-Q. Png, W.-L. Seah, J.-M. Zhuo, G.-K. Lim, *et al.*, "A general method for transferring graphene onto soft surfaces," *Nat Nano,* vol. 8, pp. 356-362, 2013.

[16] X. Liang, B. A. Sperling, I. Calizo, G. Cheng, C. A. Hacker, Q. Zhang, *et al.*, "Toward Clean and Crackless Transfer of Graphene," *ACS Nano,* vol. 5, pp. 9144-9153, 2011.

[17] T. S. Abhilash, R. De Alba, N. Zhelev, H. G. Craighead, and J. M. Parpia, "Transfer printing of CVD graphene FETs on patterned substrates," *Nanoscale,* vol. 7, pp. 14109-14113, 2015.

[18] Y. Sato, K. Takai, and T. Enoki, "Electrically controlled adsorption of oxygen in bilayer graphene devices," *Nano letters,* vol. 11, pp. 3468-3475, 2011.

[19] G. Giovannetti, P. A. Khomyakov, G. Brocks, V. M. Karpan, J. van den Brink, and P. J. Kelly, "Doping Graphene with Metal Contacts," *Physical Review Letters,* vol. 101, pp. 026803, 2008.

[20] F. Xia, V. Perebeinos, Y.-m. Lin, Y. Wu, and P. Avouris, "The origins and limits of metal-graphene junction resistance," *Nat Nano,* vol. 6, pp. 179-184, 2011.